Rev. Roum. Sci. Techn.– Électrotechn. et Énerg.
Vol. **64**, *1*, pp. 69–74, Bucarest, 2019

EFFICIENT HIGH FREQUENCY SINGLE-PHASE AC CHOPPER

MIHAI LUCANU, OVIDIU URSARU, CRISTIAN AGHION, NICOLAE LUCANU

Key words: Direct ac–ac converter, Bidirectional buck converter, Resistive or inductive load.

The paper introduces and analyzes a new single-phase ac chopper circuit with 100 kHz switching frequency. The adequate functioning and high performance of the circuit (the efficiency and the waveform of the absorbed input current and load voltage) were tested both by simulation and experimentally. Beside this wide application range, the converter size and weight are reduced, it is more efficient, responds faster in automatic control applications and the waveforms of the current supplied by the grid and of the output voltages are nearly sinusoidal.

1. INTRODUCTION

Ac choppers have numerous applications. Some of the most common are ac motor speed control, switching ac power supplies, regulated or not, voltage waveform restorers, electric heating, lighting control etc. Their performance characteristics are superior to those of the ac variators with thyristors and TRIACs.

Researchers have been focusing on ac choppers for a long time [1]. The first studies aimed at improving the power factor and at eliminating certain input current harmonics [2, 3]. In [4] is proposed a simple control scheme to bring the current from the grid in phase with the input voltage. With the increase of efficiency in power-switching devices, the efficiency of ac choppers also improved. Reference [5] presents a simple circuit with IGBTs operating at low frequency, which was tested by simulation. Three-phase power choppers were designed for three-phase ac motor speed control. Reference [6] presents a three-phase ac chopper with nine insulated gate bipolar transistors (IGBTs). Reference [7] introduces a method for assessing the efficiency of three-phase choppers.

As soon as the operating frequency of ac choppers increased, the switching of the power devices used had to be improved. This issue is analyzed in [8–10]. Three-level ac-ac converters were introduced in [11,12], as well as ac choppers with commercial modules [13]. Several concrete applications made it possible to analyze the control circuits used for ac choppers.

Reference [14] involves the use of sliding control in an ac-ac converter, while [15–17] analyze a regulated ac power supply consisting in a chopper. The use of these circuits in voltage restorers is presented in [18]. Reference [19] simplifies the construction of the magnetic component by using a common core for the coupled inductors. Reference [20] suggests the modification of the pulse width modulation (PWM) technique with the aim of improving the power factor. In [21], the authors deduce equations for the calculation of the ac-ac converter components so that the fundamental of the current supplied by the grid can be in phase with the grid voltage.

The paper presents a single-phase ac buck chopper with a new power circuit. The change of the position of two power switches allows a circuit design where only two switches are MOSs, and two switches can be bipolar transistors (BJTs), IGBTs or thyristors, although the operating frequency is high (100 kHz). According to our references, the highest switching frequency that was used was 50 kHz [18]. Moreover, the two low frequency switches become ON or OFF when the voltages and currents are zero, therefore the switching losses on the transistors are reduced and the converter efficiency improves. At the same time, these transistors, like MOSs, do not need snubber circuits. They are controlled at grid frequency. Since the output and input voltages have a common terminal, the circuit can be easily extended to the three-phase case.

The suggested solution allows the ac-ac converter to behave as two dc-dc converters that are in antiparallel connection and are supplied with variable voltage. Thus, the ac choppers efficiency can be brought to a level similar to that of the dc-dc converter. The adequate functioning of the circuit suggested was tested both by simulation and by experiments. Although the circuit requires two inductances to regulate the current, both of them can be wound on the same core in order to reduce costs. The control circuit used is simple.

The paper includes simplified equations useful for the design of the ac choppers.

2. CIRCUIT ANALYSIS

Fig. 1 presents the power circuit suggested for the single-phase ac buck chopper. The bipolar transistors T_1 and T_2 are connected in series with the current-regulating inductors L_1 and L_2 and they are controlled at the ac grid frequency. The MOSs Q_1 and Q_2 are controlled at the ac chopper switching frequency f_S. The diodes D_1 and D_2 select the adequate half-cycles of the grid, and the diodes D_3 and D_4 insure the conduction of the currents i_{L1} and i_{L2} while the MOSs are switched off.

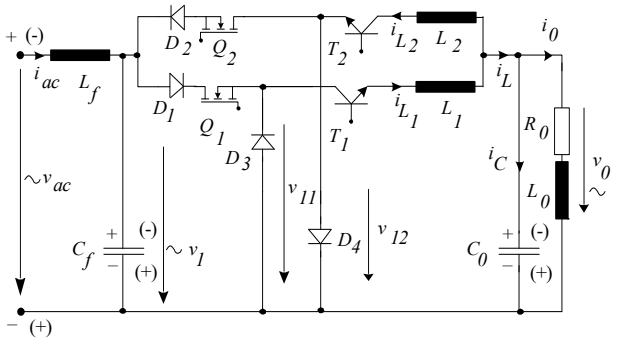

Fig. 1 – Single-phase ac buck chopper.

The grid filter contains the inductor L_f, and the capacitor C_f. The load circuit is R_0L_0, and the capacitor C_0 connected in parallel with the load has a double role: it improves the waveform of the output voltage v_o and it makes sure there is

Technical University "Gheorghe Asachi" fom Iasi, Romania, EASI Dept., E-mail: aghion@etti.tuiasi.ro

no phase shift between the voltage v_1 at the converter input and the current fundamental $i_L=i_{L1}+i_{L2}$.

Figure 2 presents the waveforms of the voltage at the converter input v_1, at the terminals of the diodes D_3 and D_4 v_{11} and v_{12}, of the currents through the regulating inductors i_{L1} and i_{L2}, of the control signals of the MOSs Q_1 and Q_2 and of the bipolar transistors T_1 and T_2.

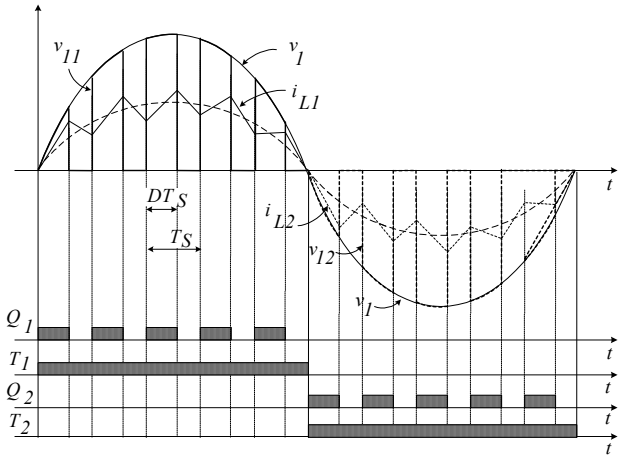

Fig. 2 – The waveforms of the voltage at the converter input v_1, at the terminals of the diodes D_3 and D_4, v_{11} and v_{12}, of the currents through the regulating inductors i_{L1} and i_{L2}, of the control signals of the MOSs Q_1 and Q_2 and of the bipolar transistors T_1 and T_2

Figure. 3 shows the control circuit, which is very simple. In the positive half-cycle of the voltage v_1, T_1 is set on, and Q_1 is controlled PWM at the switching frequency $f_S=1/T_S$, set by the sawtooth oscillator (Fig. 3). The transistors T_2 and Q_2 are switch off. In the negative half-cycle of the voltage v_1, T_2 is on, Q_2 is PWM controlled and Q_1 and T_1 are switch off. This results in two dc-dc buck converters in antiparallel connection, which, due to the diodes D_1 and D_2, are powered and in operation only during one half-cycle of the voltage v_1. With this strategy, the efficiency of ac-ac converters increases up to the efficiency level of the dc-dc converters. The PWM switching frequency f_S can be increased and efficiency is maintained.

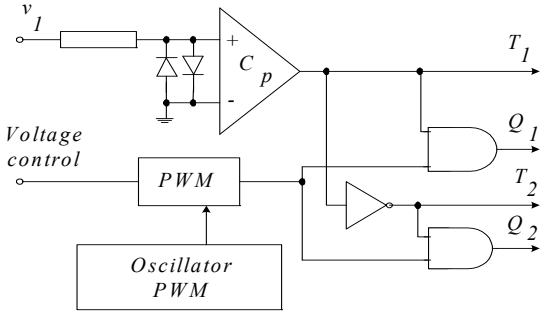

Fig. 3 – The control circuit

The PWM control of MOSs Q_1 and Q_2 is uniform with the constant duty cycle $D=\frac{t_{on}}{T_s}$. The time t_{on} is the time interval when the MOS is on, and $T_S=1/f_S$ is the switching period ($t_{on}=DT_S$). Assuming that the output voltage v_o and the load current i_o are sinusoidal, the load impedance Z and the phase shift φ between v_o and i_o are derived from the following equations:

$$Z=\sqrt{R_0^2+(\omega L_0)^2},\ \operatorname{tg}\varphi=\frac{\omega L_0}{R_0}. \tag{1}$$

The analysis below is based on the following simplifying hypotheses: the passive components and the switches are ideal and the input voltage of the converter is constant during the switching period T_S. This voltage is given by the equation:

$$v_1=\sqrt{2}V_1\sin\omega t, \tag{2}$$

where V_1 is the RMS value (approximately equal to the RMS value of the ac grid voltage), and $\omega=2\pi f$ is the angular frequency of the grid voltage (f = 50 Hz).

3. SIMPLIFIED DESIGN EQUATIONS

The design equations obtained are quite simple and accurate if we consider that the input and output voltages and load current are sinusoidal. Since the reactances of the inductances L_1 and L_2 are negligible at the ac grid frequency, we can also consider that the two voltages are in phase, so:

$$\begin{aligned} &v_1=\sqrt{2}V_1\sin\omega t, v_0=\sqrt{2}DV_1\sin\omega t\\ &i_0=\frac{\sqrt{2}DV_1}{\sqrt{R_0^2+(\omega L_0)^2}}\sin(\omega t-\varphi),\operatorname{tg}\varphi=\frac{\omega L_0}{R_0}\end{aligned} \tag{3}$$

In order for the output circuit, made up of the capacitor C_0 connected in parallel with the load R_0L_0, to behave as an equivalent resistance, the value of the capacitor C_0 must be:

$$C_0=\frac{L_0}{R_0^2+(\omega L_0)^2} \tag{4}$$

and the equivalent resistance of the output circuit is given by the equation:

$$R_{0e}=\frac{R_0^2+(\omega L_0)^2}{R}. \tag{5}$$

In the switching period k, the input and output voltages are considered constant:

$$\begin{aligned} &v_{1k}=\sqrt{2}V_1\sin\omega t_k, v_{0k}=\sqrt{2}DV_1\sin\omega t_k\\ &t_k=(k-1)T_S+\frac{1}{2}T_S, k=\overline{1,m_f}, m_f=\frac{f_S}{f_{grid}}=\frac{10^5}{50}=2\cdot10^3\end{aligned} \tag{6}$$

and the other parameters of the converter comply with the equations of the ideal buck converter.

We assume that, in a given application, the input voltage varies within these limits:

$$V_{1(\min)}\le V_1\le V_{1(\max)} \tag{7}$$

and the output voltage must be subject to control within the following limits:

$$V_{0(\min)}\le V_0\le V_{0(\max)}\cdot \tag{8}$$

Under these conditions, the duty cycle should vary within the following limits:

$$D_{(\min)} \le D \le D_{(\max)}, D_{(\min)} = \frac{V_{0(\min)}}{V_{1(\max)}}, D_{(\max)} = \frac{V_{0(\max)}}{V_{1(\min)}}. \quad (9)$$

The ripple current through the inductors L_1 and L_2 is calculated as follows:

$$\Delta i_{Lk} = D(1-D)\frac{v_{1k}}{Lf_s} \quad (10)$$

and the average current through these inductors (as well as through the transistors T_1 and T_2) is:

$$I_{Lk\,AVR} = \frac{v_{0k}}{R_{0e}} = \frac{DR_0 v_{1k}}{R_0^2 + (\omega L_0)^2}. \quad (11)$$

The maximum peak to average current ripple through the inductors L_1 and L_2 is:

$$\left(\frac{\Delta i_{Lk}}{I_{Lk\,AVR}}\right) = \frac{\left[1 - D_{(\min)}\right]\left[R_0^2 + (\omega L_0)^2\right]}{R_0 L f_s}. \quad (12)$$

This equation is used for the design of the inductances L_1 and L_2. For this purpose, we can either set a certain percentage as the normalized ripple or establish that the percentage should not exceed 50 % if we use the converter continuous conduction mode.

The RMS currents through the inductor L_1 and the transistor T_1 (as well as through L_2 and T_2) is:

$$I_{Lk\,RMS} = I_{T1k\,RMS} = Dv_{1k}\sqrt{\left(\frac{1}{R_{0e}^2}\right)^2 + \frac{1}{12}\left(\frac{1-D}{Lf_s}\right)^2}. \quad (13)$$

The average current (AVR) through the MOS Q_1 and the diode D_1 (therefore through Q_2 and D_2 too) is:

$$I_{Q1k\,AVR} = I_{D1k\,AVR} = \frac{D^2 v_{1k}}{R_{0e}}. \quad (14)$$

The RMS current through the MOS Q_1 and the diode D_1 (therefore through Q_2 and D_2 too) is:

$$I_{Q1k\,RMS} = I_{D1k\,RMS} = D\sqrt{D}\, v_{1k}\sqrt{\frac{1}{R_{0e}^2} + \frac{1}{12}\left(\frac{1-D}{Lf_s}\right)^2}. \quad (15)$$

The average and RMS currents through the diode D_3 (equal to the ones passing through D_4) are:

$$I_{D3\,AVR} = \frac{D(1-D)v_{1k}}{R_{0e}}.$$
$$I_{D3\,RMS} = D\sqrt{1-D}\, v_{1k}\sqrt{\frac{1}{R_{0e}^2} + \frac{1}{12}\left(\frac{1-D}{Lf_s}\right)^2}. \quad (16)$$

The maximum repetitive currents through the inductors, MOSs, bipolar transistors and diodes are:

$$I_{LRM} = I_{Q1RM} = I_{D1RM} = I_{T1RM} = I_{D3RM} = \frac{Dv_{1k}}{R_{0e}} + \frac{D(1-D)v_{1k}}{2Lf_s} = Dv_{1k}\left(\frac{1}{R_{0e}} + \frac{1-D}{2Lf_s}\right) \quad (17)$$

The voltage stress on the MOSs and diodes is:

$$V_{Q1RM} = V_{D1RRM} = V_{D3RRM} = v_{1k}. \quad (18)$$

The voltage stress on the bipolar transistors is:

$$V_{T1RM} = V_{T2RM} = v_{0k} = Dv_{1k}. \quad (19)$$

Considering that v_{1k} varies sinusoidally and that all the components are in conduction only in one half-cycle of the grid voltage, we can establish the maximum values of the current and voltage stress.

The maximum values of the average currents through the inductors and the bipolar transistors result from equation (11):

$$I_{L1\,AVR} = I_{L2\,AVR} = I_{T1\,AVR} = I_{T2\,AVR} = \frac{D_{\max}\sqrt{2}V_{1(\max)}}{\pi R_{0e}}. \quad (20)$$

The maximum values of the RMS currents through the inductors and the bipolar transistors result from equation (13):

$$I_{L1\,RMS} = I_{L2\,RMS} = I_{T1\,RMS} = I_{T2\,RMS} = D_{(\max)}V_{1(\max)}\sqrt{\frac{1}{2}\left(\frac{1}{R_{0e}}\right)^2 + \frac{1}{24}\left(\frac{1-D_{(\max)}}{Lf_s}\right)^2}. \quad (21)$$

The maximum values of the average currents through the MOSs Q_1 and Q_2 and through the diodes D_1 and D_2 result from equation (14):

$$I_{Q1\,AVR} = I_{Q2\,AVR} = I_{D1\,AVR} = I_{D2\,AVR} = \frac{D_{(\max)}^2\sqrt{2}V_{1(\max)}}{\pi R_{0e}}. \quad (22)$$

The maximum values of the RMS currents through MOSs Q_1 and Q_2 and through diodes D_1 and D_2 are, according to equation (15):

$$I_{Q1\,RMS} = I_{Q2\,RMS} = I_{D1\,RMS} = I_{D2\,RMS} = D_{(\max)}\sqrt{D_{(\max)}}V_{1(\max)}\sqrt{\frac{1}{2R_{0e}^2} + \frac{1}{24}\left(\frac{1-D_{(\max)}}{Lf_s}\right)^2}. \quad (23)$$

The maximum voltage stress on the MOSs and diodes results from equation (18):

$$V_{Q1RM} = V_{Q2RM} = V_{D1RRM} = V_{D2RRM} = V_{D3RRM} = V_{D4RRM}\sqrt{2}V_{1(\max)}. \quad (24)$$

The maximum voltage stress on the bipolar transistors results from equation (19):

$$V_{T1RM} = V_{T2RM} = D_{(\max)}\sqrt{2}V_{1(\max)}. \quad (25)$$

4. SIMULATION AND PROTOTYPE RESULTS

The adequate operation of the circuits presented was tested by simulation. In all the circuits, the converter was powered by a voltage v_1 = 110 V, f_m = 50 Hz. The load used in the simulations and in the prototype is the same: resistive load: R=65 ohm; inductive load: R=65 ohm and L=30 mH.

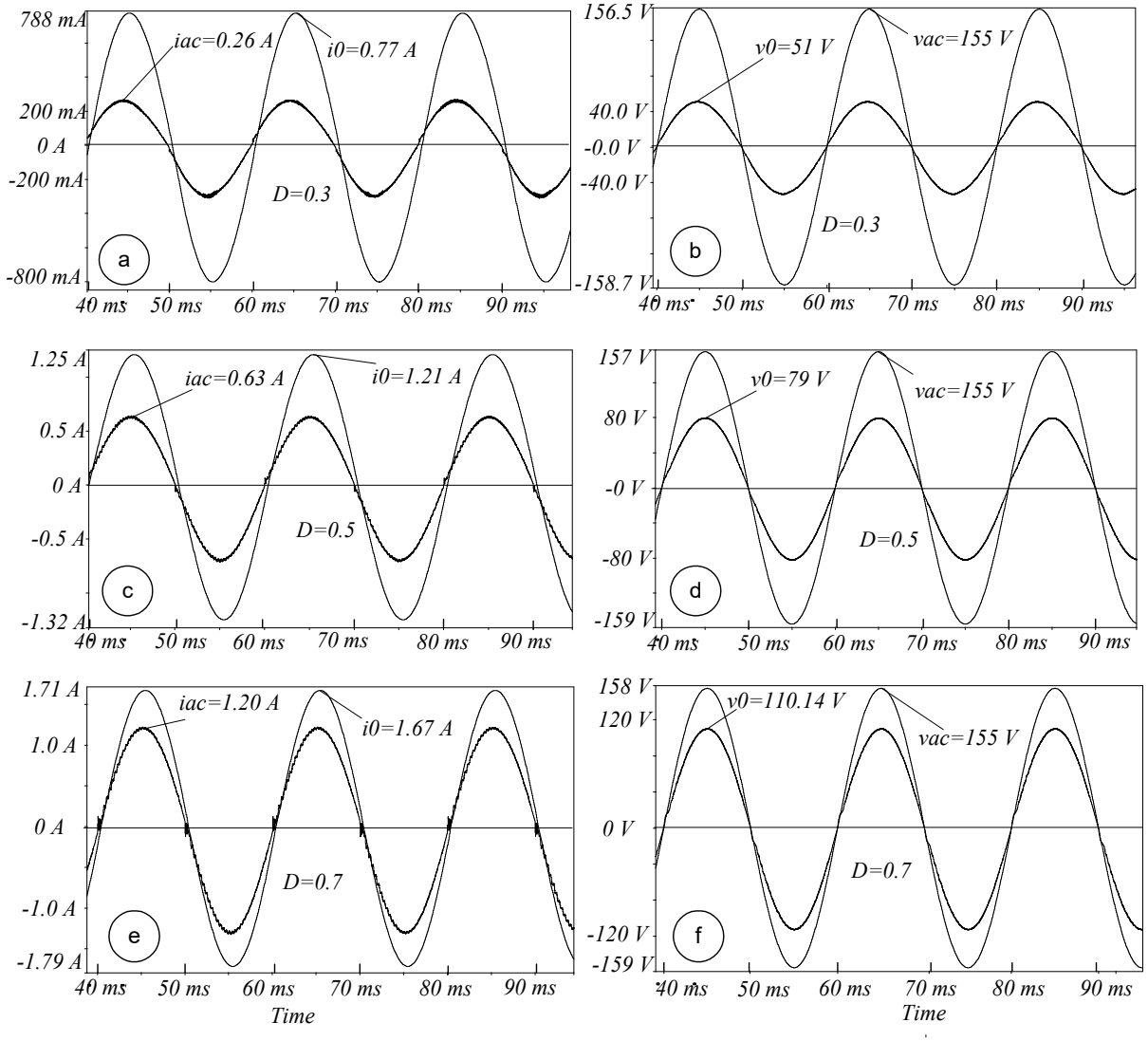

Fig. 4 – Waveforms obtained by simulations in the case of the inductive load L=30 mH, R=65 ohm, of the input current i_{ac}, output current i_0, input voltage v_{ac} and output voltage $v_{0,}$ for a duty cycle D=0.3 (a) and (b), D=0.5 (c) and (d) and D=0.7 (e) and (f).

Table 1 presents the component values used for the prototype.

Table 1

Component values used for the prototype

Parameters	Symbol	Value
ac input voltage	V_m	110 V (RMS)
Input frequency	f_m	50 Hz
Resistive load	R	65 Ω
Inductive Load	R/L	65 Ω / 30 mH
Transistors	Q_1-Q_2	SPP20N60C3
Transistors	T_1-T_2	2SC5793
Diodes	D_1-D_4	MURF1620CT
Inductances	L_1, L_2	0.25 mH
Input filter	L_f	1 mH
	C_f	0.5 µF
Microcontroller	µC	PIC32MX695F512L
PWM frequency	f_S	100 KHz

Figure 4 shows waveforms obtained by simulations in thecase of the inductive load L= 30 mH, R = 65 ohm, of the input current i_{ac}, output current i_0, input voltage v_{ac} and output voltage $v_{0,}$ for a duty cycle D = 0.3 (a) and (b), D = 0.5 (c) and (d) and D = 0.7 (e) and (f).

The laboratory prototype presented in Fig. 5 was built and tested with the following parameters: input voltage v_{ac} = 110 V and f_m = 50 Hz. The components of the power supply filter are: L_f =1 mH, C_f = 0.5 µF and the switching frequency is f =100 kHz. The control circuit of the converter was made up using a PIC32MX695F512L microcontroller, made by the MICROCHIP Company.

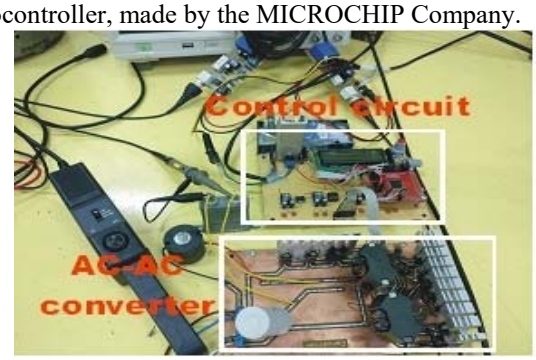

Fig. 5 – Experimental setup.

Figure 6 shows the waveforms obtained by measurement in the case of inductive load L=30 mH, R=65 ohm, of the input current i_{ac}, output current i_0, input voltage v_{ac} and output voltage $v_{0,}$ for a duty cycle D=0.3 (a) and (b), D=0.5 (c) and (d) and D=0.7 (e) and (f).

For calculating the THD, the following equation was used:

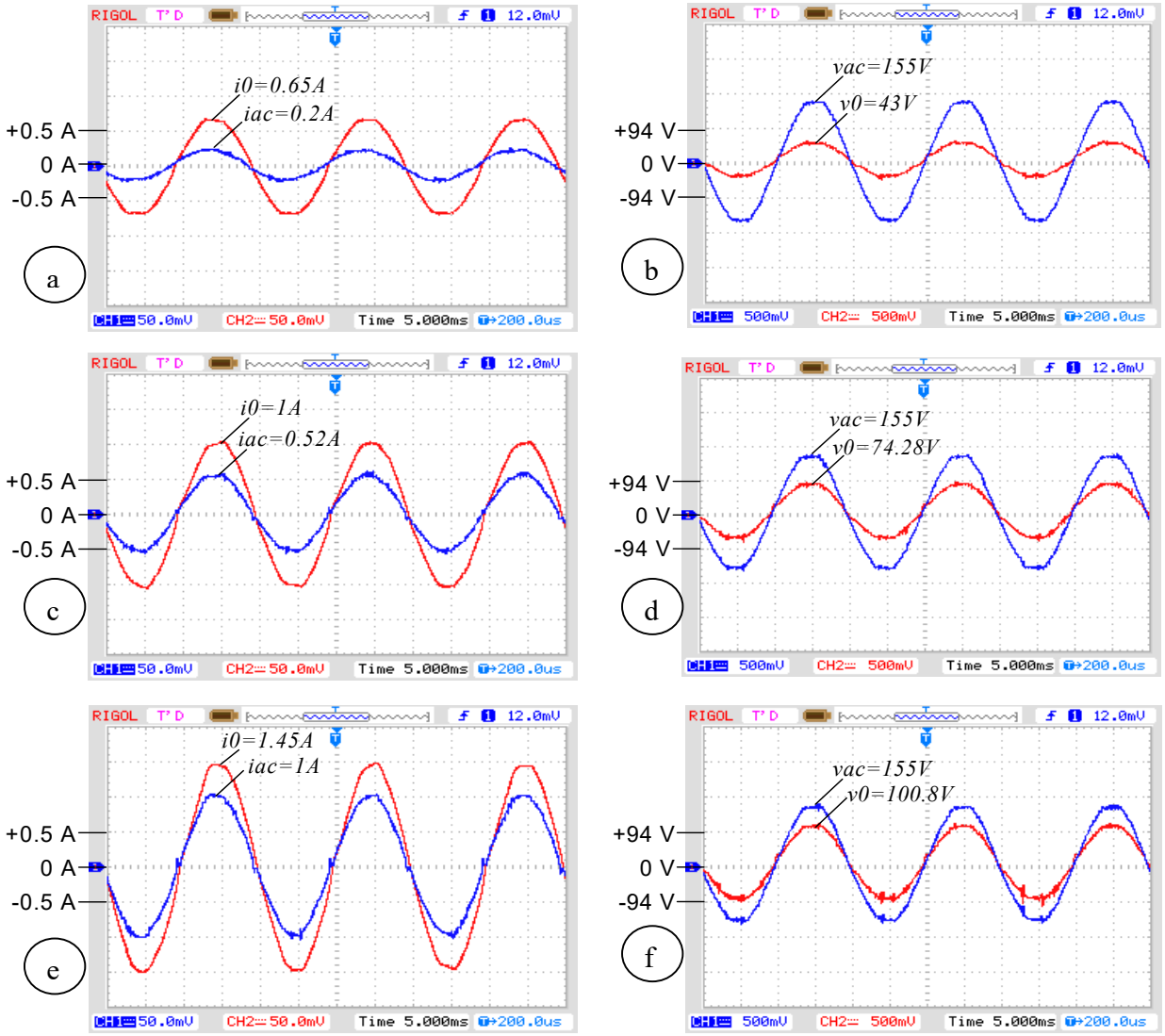

Fig. 6 – Waveforms obtained by measurement in the case of the inductive load L=30mH, R=65 ohm, of the input current i_{ac}, output current i_0, input voltage v_{ac} and output voltage v_0, for a duty cycle D=0.3 (a) and (b), D=0.5 (c) and (d) and D=0.7 (e) and (f).

$$THD = \frac{\sqrt{I_{ac2}^2 + I_{ac3}^2 + I_{ac4}^2}}{I_{ac1}} \quad (26)$$

where I_{ac1} is the RMS value of the power supply fundamental, I_{ac2} is the RMS value of the first harmonic of the power supply at a switching frequency of 100 kHz, etc.

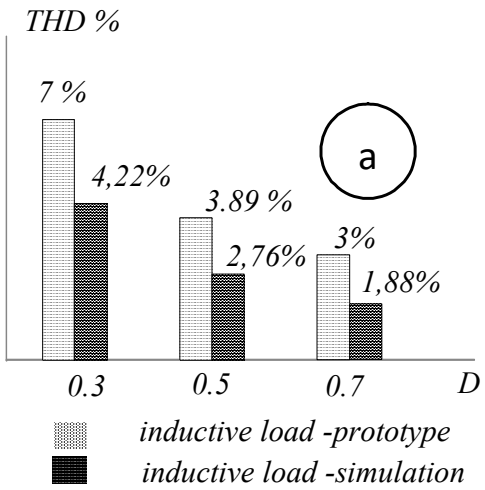

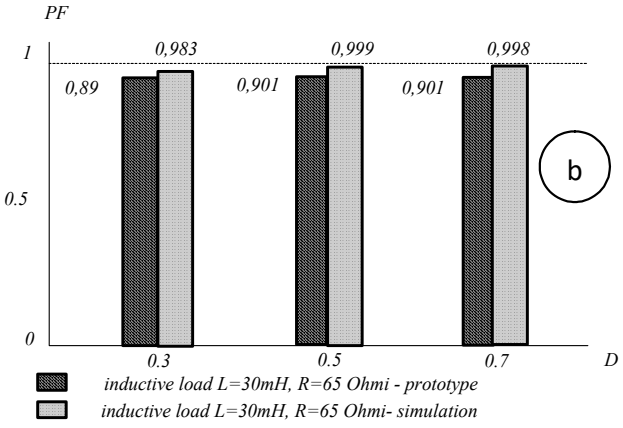

Fig. 7 – (a) THD for inductive load case and (b) Power Factor for inductive load case

Figure 7a shows the THD for the inductive load case. Fig. 7b compares (simulation *vs.* prototype) the PF analyses of the current supplied by the power supply, for the inductive load case.

The efficiency, calculated based on the waveforms from Fig. 6e and Fig. 6f for D = 0.7, is 94 % as compared to the highest values reported (in [7] – 90 % and in [14] – 92 %)

at 100 kHz switching frequency, which is twice more than the 50 kHz maximum frequency in reference [18] and the 25 kHz frequency in reference [14]. The THD values for the grid current and the output voltage are comparable to those of the reference choppers.

5. **CONCLUSION**

The paper analyzes a new efficient high frequency single phase ac chopper with two MOSs and two bipolar transistors (BJTs). BJTs were used in order to prove that these devices should not be chosen according to the functioning frequency, but depending on conduction losses and costs. For switch control, we used constant sampling, with the same duty cycle in all the switching periods and no dead time. The input filter is simple and the input current waveform is adequate. Although the circuit proposed is single-phase, a three-phase converter can be easily obtained by joining three single-phase converters.

ACKNOWLEDGMENT

This work was supported by a research grant of the TUIASI, project number 0122 (TUIASI-GI-2018-0122).

Received on February 21, 2019

REFERENCES

1. G.N. Rivenkar, D.S. Transi, *Symmetrical pulse width modulated A.C. chopper,* I.E.E.E. Trans. Ind. Electron. Contr. Instrum., 1977, I.E.C. 1-24, pp. 41-45.
2. A. Boudouda, N. Boudjerda, A. Aibeche, *Dual randomized pulse width modulation technique for buck converter fed by photovoltaic source*, Rev. Roum. Sci. Techn.-Electrotechn. Et Energ. **63**, 3, pp. 289-294, 2018.
3. Do Ifyum, G. H. J. Choe, M., Chosany, *Asymmetrical PWM technique with harmonic elimination and power factor control in A.C. chopper* I.E.E.E. Trans. Power Electron., 1995, **10**, pp. 175-184.
4. S. Komeda, H. Fujita, *A phase-shift-controlled direct ac-to-ac converter for induction heaters*, I.E.E.E. Trans. Power Electron., 2018, **5**, pp. 4115-4124.
5. M. Derick, P. A. Athira, M. Bincy, *Modified Single Stage ac-ac Converter* International Journal of Power Electronics and Drive System (IJPEDS), **6**, *1*, pp. 1-9, 2015.
6. L. Congwei, W. Bin, N.R. Zargari, X. Devei, W. Jiacheng, *A novel three-phase leg A.C./A.C. converter using nine I.G.B.T.'s* I.E.E.E. Trans. Power Electron., 2009, **24,** *5*, pp. 1151-1160.
7. R. Lai, F. Wang, R. Burgos, *A systematic topology evolution methodology for high-density three-phase PWM A.C./A.C. converters*, I.E.E.E. Trans. Power Electron., 2008, **23**, *6*, pp. 2665-2680.
8. Y.H. Kim, B.D. Min, B.H. Kwon, S.C.Won, *A PWM buck-boost A.C. chopper solving the commutation problem* I.E.E.E. Trans. Ind. Electron. , 1998, **45**, *5*, pp. 832-835.
9. C. Petrescu, C. Vatavu, I. Zaharia, *Power analysis of single-phase nonlinear loads in accordance with IEEE standards based on real time signal recordings*, Rev. Roum. Sci. Techn.-Electrotechn. Et Energ. **61**, *3*, pp. 227-232, 2016.
10. M. Lucanu, O. Ursaru, C. Aghion and N. Lucanu, *Single-phase direct A.C./A.C. step-down converter*, I.E.T. Power Electron., **7**, *12*, 2014, pp. 1-9.
11. J. D. Yang , L. Li, K. M. Yang, *A novel buck-boost mode single stage three lavel A.C./A.C*, Converter Proc. I.E.E.E. Indus. Electron. (I.E.C.O.N.), 2008, pp. 596 – 600.
12. K. Georgakas and A. Safacas, *Modified sinusoidal pulse-width modulation operation technique of on A.C./A.C. single-phase converter to optimize the power factor*, I.E.T. Power Electron., 2011, **3**, *3*, pp. 454-464.
13. T.B. Soliero, C.A. Petry, J.C. Dos, S. Fagundes, Y. Barbi, *Direct A.C./A.C. converters using commercial power modules applied to voltage restorers*, I.E.E.E. Trans. Ind. Electron., 2011, **58**, *1*, pp. 278-288.
14. L. Garsia de Vicuna, M. Castilla, J. Miret, J. Matas, J. M. Guerrero, *Sliding-mode control for a signal phase A.C./A.C. quantum resonant converter* I.E.E.E. Trans. Ind. Electron., 2009, **56**, *9*, pp. 3496-3504.
15. C. Y. Park, Y. M. Kwon, B.H. Kwon, *Automatic voltage regulator based on series voltage compensation with A.C. chopper source*, I.E.T. Power Electron., 2012, **5**, *6*, pp. 719-725.
16. C. M. Wang, C. H. Lin, C. H. Su, S. Y. Chang, *A novel single-phase soft-switching ac chopper without auxiliary switches*, I.E.E.E Trans. Power Electron., 2011, **26**, *7*, pp. 2041-2048.
17. D. Chen, Y. Chen, *Step-up ac voltage regulators with high frequency link,* I.E.E.E Trans. Power Electron., 2012, 28, pp. 390-397.
18. Rosas-Caro, J.C., Mancilla-David, F., Ramisez-Arredondo, J.M., Bakir, *Two-Switch, three-phase A.C.-link dynamic voltage restorer*, I.E.T. Power Electron., 2012, **5**, *9*, pp. 1754-1763.
19. S. Kim, D. Jang, H.G. Kim, H. Cha*, Cascaded dual-buck ac-ac converter using coupled inductors,* The 2018 International Power Electronics Conference, pp. 2619-2624.
20. A. Aurasopon, W. Khamsen, *Improvement of input power factor in PWM A.C. choppers selecting the optimal parameters*, Przeghed Elektrotechiczny, I.S.S.N. 0033-2097, 2013, 89, pp. 210-216.
21. L. Li, Y. Yang, Q. Zhong, *Novel family of single-stage three level A.C. Choppers*, I.E.E.E Trans. Power Electron., 2011, **26**, *2*, pp.504-511.